JOURNAL OF MATERIALS SCIENCE 16 (1981) 2977–2987

Micromechanics and kinetics of deformation zones at crack tips in polycarbonate

ATHENE M. DONALD, EDWARD J. KRAMER
Department of Materials Science and Engineering and the Materials Science Center, Cornell University, Ithaca, NY 14853, USA

Plane stress deformation zones are grown from cracks produced by electron beam irradiation in thin films of polycarbonate (PC) bonded to ductile copper grids. The kinetics of zone growth in both length and width are followed by optical microscopy while v_f, the ratio of zone thickness to film thickness, is followed by optical interference and transmission microscopy measurements. These data allow the zone surface displacement and stress profiles to be computed at various times during growth. There is a stress concentration at the zone tip which relaxes to a uniform stress over the rest of the zone up to near the crack tip. Both the tip stress concentration and uniform zone stress decrease as zone growth proceeds. The zone surface displacement rate follows these changes in stress. It is highest just behind the zone tip where the stress concentration exists and is constant in the uniform stress zone. It decreases markedly with time. While the Dugdale model does not predict the details of the zone micromechanics, in particular the zone tip stress concentration, it does predict qualitatively the correct trends. The crack propagates into the oriented polymer in the deformation zone in the form of a characteristic half diamond shape, which is the analogue of diamond cavities previously observed in the fracture process of oriented bulk polymers.

1. Introduction

In a preceding paper [1] the formation of plane stress deformation zones (DZs) at crack tips in annealed thin films of polycarbonate (PC) have been described. These large, well-defined DZs are ideal subjects for a study of the kinetics of zone thickening and lengthening. Attempts by previous workers [2–4] to observe craze growth by optical microscopy and to compare their results with theoretical models such as the Dugdale model [5] have been limited by the resolution of the light microscope and the small dimensions of the craze, plus the necessity to assume that the refractive index along the craze is constant.

For the case of the DZs described here the last two difficulties have largely been overcome. Because of the similarity of the mechanism of zone thickening to craze thickening the zones should provide good models for craze growth. In this paper the experimental results on zone growth kinetics and micromechanics are described and a comparison with both the Dugdale model for a plastic zone at a crack tip, and with craze growth is described. The nature of crack propagation into the DZs is also discussed.

2. Experimental procedure

Thin films of polycarbonate (GE Lexan™ grade 130, specific viscosity, $[\eta] = 0.665\ \mathrm{dl\,g^{-1}}$, kindly supplied by Dr Roger Kambour) were cast from solution. These films were bonded to annealed copper grids, which had been precoated with PC, by exposure to methylene chloride vapour. After the films had been placed in a vacuum overnight, to remove excess solvent from the film, a static crack was introduced by irradiation with the intense electron beam of a JEOL 733 Superprobe. Subsequently the films were annealed for 1 h at 132° C prior to straining. Further details of the method of specimen and crack preparation may be found in [1].

Time-lapse photography through a conventional optical microscope may be used to monitor changes

0022–2461/81/112977–11$03.10/0

in length and width as growth of a DZ at a crack tip proceeds at constant applied strain. To obtain the displacement profile, $w(x)$, these measurements can be combined with transmission electron microscopy (TEM) measurements of v_f (where v_f is the ratio of the thickness of the material within the DZ to the thickness of the surrounding film) obtained from Equation 1 of [1].

3. Analysis of DZ micromechanics

Since the v_f measurements obtained by electron microscopy of these zones (when growth is complete) show little variation with position in the zone [1], it seems reasonable to assume that creep of the already deformed material makes a negligible contribution to zone thickening as zone growth proceeds. Surface drawing has been shown to be the dominant mechanism for dry crazes in both PS [6,7] and PC [8], and for the system studied here, the incorporation of fresh material into the zone can be observed directly by viewing the position of dust particles within the film relative to the edge of the DZ. It is assumed therefore that v_f is essentially constant throughout zone growth (i.e. at all times $v_f = 0.71$). Hence, by using the relationship [6]

$$w(x) = \tfrac{1}{2}\tau(x)(1 - v_f), \tag{1}$$

where τ is the measured zone thickness, the surface displacements $w(x)$ of the zone can be obtained as growth proceeds.

The measured profiles can be compared with the prediction of the Dugdale model [5,9] for a plastic zone at a crack tip. The basic assumption of this model is that the surface stress is constant over the entire plastic zone. The displacements w are derived from the equation

$$w(\beta) = \frac{aS_c}{\pi E^*} H(\beta,\beta_c), \tag{2}$$

where $\beta = \arccos(x/a)$ and $\beta_c = \arccos(a_0/a)$. Here x is the distance from the centre of the crack, a is half the total crack plus plastic zone length, a_0 is half the crack length and S_c is the constant surface stress of the plastic zone. The function $H(\beta,\beta_c)$ is given by

$$H(\beta,\beta_c) = \cos\beta \ln\left[\frac{\sin^2(\beta_c - \beta)}{\sin^2(\beta_c + \beta)}\right] + \cos\beta_c \ln\left[\frac{(\sin\beta_c + \sin\beta)^2}{(\sin\beta_c - \sin\beta)^2}\right] \tag{3}$$

and an effective Young's modulus E^* is defined by

$$E^* = \begin{cases} E/1 - \nu^2 & \text{for plane strain} \\ E & \text{for plane stress} . \end{cases} \tag{4}$$

For a given a and a_0, S_c can be found from the requirement that there is no stress singularity at the crack tip. This calculation yields

$$S_c = \frac{\pi\sigma_\infty}{2\beta_c}, \tag{5a}$$

where σ_∞ is the applied stress.

For this system a and a_0 can be measured diriectly from the optical micrographs at all stages of zone growth, and so the predicted form of w can be derived for all times for the particular geometry observed, if σ_∞ is known. Equivalently, since the displacement w_0 in the centre of the crack (at $x = 0, \beta = \pi/2$) is conveniently measured by optical microscopy one can find S_c from Equation 2 as

$$S_c = \frac{\pi E^* w_0}{aH(\pi/2,\beta_c)} . \tag{5b}$$

Although σ_∞ can be estimated from the strain applied to the grid, this estimate inevitably neglects the stress relaxation due to the opening of crack and zone in the finite grid square as well as the anelastic stress relaxation in the film itself. In that sense Equation 5b provides a more accurate estimate, a point which is confirmed by the fact that the displacements predicted using this value of S_c match the experimental displacements measured in the crack and the plastic zone near the crack tip well, whereas those predicted using the σ_∞ computed from the applied strain were ~30% too large. Therefore Equation 5b was used to obtain S_c and Equation 5a was used to compute σ_∞ from this S_c. Using the known $w(x)$ profile along the zone and the Fourier transform method developed from the work of Sneddon [10] by Lauterwasser and Kramer [6], the actual surface stress profile $S(x)$ can be calculated from the equations

$$S(x) = \Delta S(x) + \sigma_\infty \tag{6a}$$

and

$$\Delta S(x) = -\frac{2}{\pi}\int_0^\infty \bar{p}(\xi)\cos(x\xi)\mathrm{d}\xi \tag{6b}$$

with

$$\bar{p}(\xi) = \frac{\xi E^*}{2}\int_0^a w(x)\cos(x\xi)\mathrm{d}x. \tag{6c}$$

This method requires that the displacements along the crack are known, as well as along the DZ. These crack displacements are calculated from the Dugdale model (using the known a, a_o and the computed S_c) and are joined smoothly to the $w(x)$ measured in the DZ. As mentioned above the experimentally measured and computed values of w agree in the crack, but since one can show theoretically that the displacements in the crack must be very close to those of the Dugdale model for any reasonable variation of $S(x)$ over the zone, the computed $w(x)$ values are used in the crack to avoid introducing unnecessary artifacts in $S(x)$ due to the experimental measuring error in $w(x)$.

In this method it is assumed that v_f can be taken as a constant. Close to the zone tip it has been shown [1] that v_f increases from its average value towards 1. Thus the surface displacements at the zone tip will be an overestimate if this increase in v_f is not allowed for. Similarly, near the crack tip v_f decreases from its average value of 0.71 to 0.5. These deviations from the average v_f can only be accurately determined by TEM when growth is complete. A comparison of the $w(x)$ profile for such a terminal DZ computed with the actual v_f values with that computed using a constant v_f of 0.71 shows that the errors are only significant near the DZ tip when the absolute displacement is $\lesssim$100 nm. The main effect of this correction is to decrease slightly the absolute magnitude of the stress concentration at the zone tip. At the crack tip the experimental $w(x)$ profile is joined to the computed $w(x)$ profile of the crack at the point of maximum zone width (which occurs just ahead of the crack tip). The region ($\sim 4\,\mu$m long) just ahead of the crack to this point of maximum zone width is excluded from the analysis. It is in this region that v_f decreases (leading to an increased displacement despite the decrease in zone thickness τ). Because of this exclusion little error is introduced around the crack tip because of the deviation of v_f from the average.

4. Results

4.1. Observations on zone growth

For the specimen shown in Fig. 1, micrographs were taken at increasing intervals of time from 35 sec to 1 h after the strain of 2.5% was initially applied. Fig. 2a shows a plot of zone length against $\ln t$ for the specimen; Fig. 2b shows the ratio of maximum displacement to zone length against $\ln t$. It can be seen that the zone growth fits a logarithmic growth law well, but over the relatively short time of the experiment it is not possible to differentiate between logarithmic and power-law growth, the latter fitting the experimental date equally well. Verheulpen-Heymans and Bauwens [11] have shown that isolated crazes in PC grow linearly with log time, and that the ratio of craze width to length is essentially constant throughout growth. These results on zone growth therefore suggest a similar growth law to crazes, but the thickening kinetics would seem to be different from those for isolated crazes grown under constant load.

Using the analytical method described in the previous section, the displacement profiles $w(x)$ for the zone can be obtained throughout growth. A comparison of the $w(x)$ profile for $t = 50$ sec and 60 min with the $w(x)$ profile predicted by the Dugdale model is shown in Fig. 3a and b. The form of these is typical of all other times. It is obvious that the Dugdale model does not predict the correct form of the displacement profile; it underestimates the displacement along the zone at all points and at all times.

The surface stress profiles $S(x)$, obtained from the $w(x)$ profiles of Fig. 3a and b, via Equations 6a to c, are shown in Fig. 4a and b. It can be seen that along the majority of the zone the stress is approximately constant $S = \langle S \rangle$ and drops with

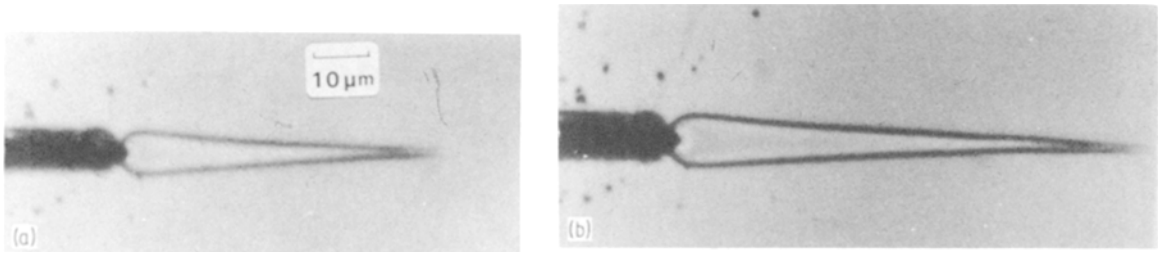

Figure 1 (a) Appearance of a deformation zone at a crack tip in annealed PC 40s after straining, (b) the same zone as in Fig. 1a at 60 min after straining.

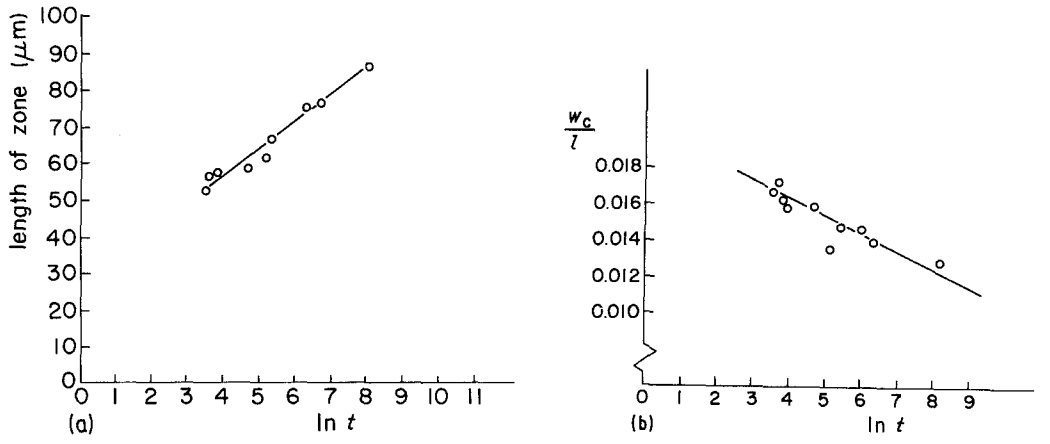

Figure 2 (a) DZ length against ln time, (b) the ratio of maximum zone displacement to zone length against ln time.

time ($\langle S \rangle = 44$ MPa at $t = 40$ sec compared with 42 MPa at $t = 3600$ sec). However it falls below the constant surface stress value predicted by the Dugdale model ($S_c = 52.5$ MPa at $t = 40$ sec and 48 MPa at $t = 3600$ sec), reflecting the more gradual gradient of the displacement profile dw/dx obtained experimentally. This relation between dw/dx and the surface stress is most easily seen from the "distributed dislocation theory" due to Bilby and Eshelby [12]. In their model the local stress $S(x)$ is proportional to $\int_0^a [w'/(x-x')]\,dx'$, which is strongly weighted to the local value of the gradient $w' \equiv dw/dx$. Since the overall gradient experimentally obtained is lower than that predicted, a lower surface stress is to be expected.

At the zone tip there is a sharp drop in the displacement (i.e. a sudden increase in dw/dx), and this increase is reflected in the stress concentration which exists at the zone tip, as seen in Fig. 4a and b. As discussed in the previous sections, the absolute magnitude of the stress concentration cannot be reliably obtained because of uncertainties in v_f at the zone tip but the results suggest the stress concentration drops with time.

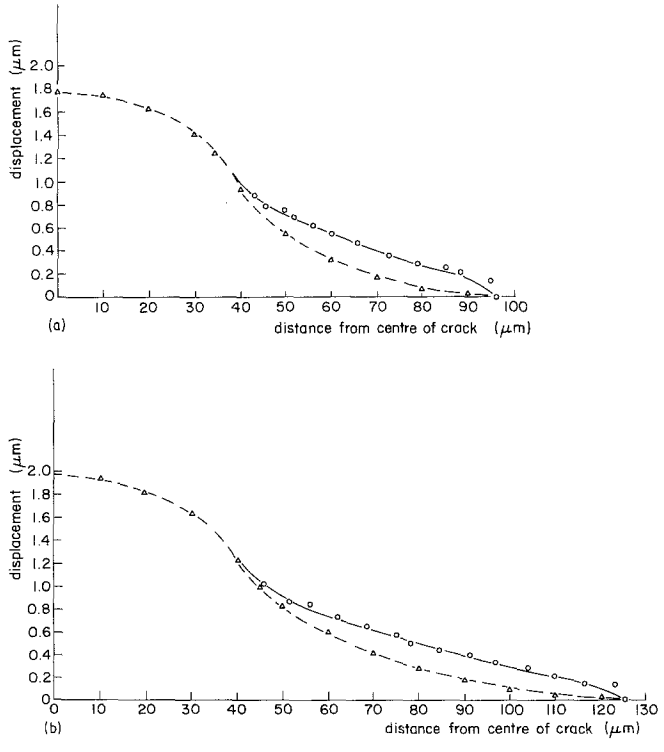

Figure 3 A comparison of the experimentally obtained displacement profiles $w(x)$ (solid line) with those predicted by the Dugdale model (dotted line): (a) at $t = 40$ sec and (b) at $t = 60$ min.

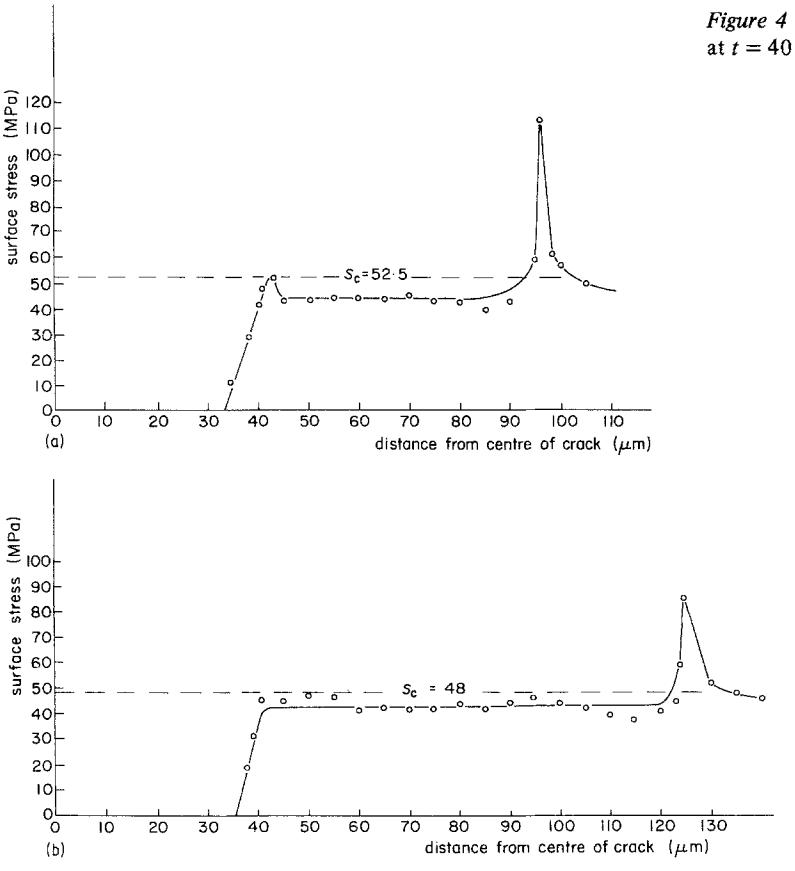

Figure 4 The surface stress profile $S(x)$: (a) at $t = 40$ sec and (b) at $t = 60$ min.

These results on the surface stress profiles along a DZ closely parallel the form of those obtained previously for crazes grown from crack tips in PS [7]. Here too, an approximately constant surface stress was obtained along the majority of the craze, with an average value below that predicted by the Dugdale model. A stress concentration was found at the craze tip.

4.2. Analysis of the surface displacement rate

From the displacement profiles calculated during growth, the displacement rate along the zone can be estimated by considering the change in displacement at each point over the time interval between photographs. The results of this analysis are shown in Fig. 5. Two curves are plotted, one yielding the displacement rate averaged over the time interval from 40 to 230 sec and the second averaged over 230 to 3600 sec. Such large time intervals are necessary to ensure reasonable accuracy.

Three conclusions can be drawn from these curves. Firstly, over the majority of the zone, where S is constant, the displacement rate is also roughly constant. Secondly, the displacement rate decreases markedly with increasing time from zone initiation. Finally, the displacement rate increases at the zone tip. These results suggest a model for surface drawing of fresh material into the zone at a rate which is dependent on the surface stress.

Over the majority of the zone the stress is well approximated by a constant, as in the Dugdale model, and consequently the displacement rate is also constant here. As the average stress drops during growth, the rate of surface drawing decreases rapidly. Although the surface stress calculations show only a total drop of ~5% in the average surface stress along the zone as growth proceeds the displacement rate drops by two orders of magnitude from a mean rate of 3 to 4Å sec^{-1} at the earlier time, to 0.04Å sec^{-1}. Near the zone tip a stress concentration exists and here a sharp peak in the displacement rate is observed. The height of this peak drops with time which is consistent with the suggestion that the magnitude of the stress concentration is also diminishing.

It has been suggested [6,13] that the drawing of fresh material from the bulk into a craze may

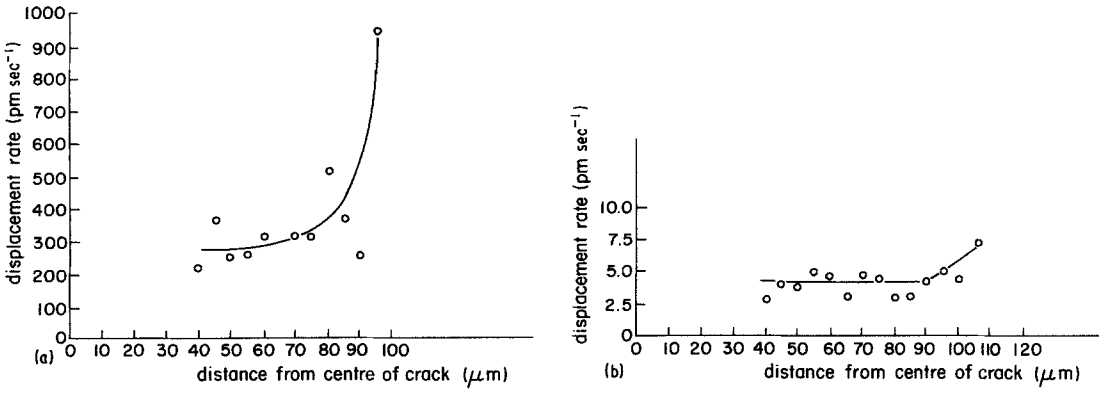

Figure 5 Displacement rate against position along the zone averaged (a) over the time interval 40 to 230 sec and (b) over the time interval 230 to 3600 sec.

occur by a mechanism similar to neck propagation in fibres and bulk specimens. For neck propagation with constant shape, the propagation rate, v_n, in monofilaments has been shown to follow an equation of the Eyring form [14, 15] i.e.

$$v_n = v_o \exp \frac{A\tau_p}{k_B T}, \quad (7)$$

where τ_p is the propagation shear stress, k_B is the Boltzmann constant, T is the absolute temperature and A and v_0 are constants. Verheulpen-Heymans [13] has used this idea to model craze thickening and to derive typical fibril diameters for PC crazes assuming a constant neck shape corresponding to a steady-state neck velocity. However, since both the observed neck propagation and craze thickening rates in PC are decreasing functions of time, this assumption is unlikely to be valid [14]. Experiments are currently in progress to examine the shape of the "neck" at the DZ–matrix interface in the specimens described here.

A second limitation of Verheulpen-Heymans model arises because she was not able to measure the local surface stress. In the experiments described here it has been possible to verify directly that the surface displacement rate of the zone is dependent on the local surface stress.

Because of the increase of v_f near the zone tip the shape of the "neck" at which drawing occurs is not the same as that adjacent to the "mature" (constant v_f) portion of the zone. Since the local stresses and strain rates in the drawing neck depend on this shape one cannot at this point interpret the link between the surface stress increase and the displacement rate increase at the zone tip more quantitatively. Nevertheless there seems to be a close analogy between neck propagation and the phenomenon of zone thickening.

As shown in Fig. 2, the ratio of maximum zone displacement to length decreases with time, which means that the rate of zone thickening by surface drawing decreases more than the rate of tip advance as the zone grows. It is of interest to note that this inequality is in qualitative agreement with the predictions of the Dugdale model. This prediction follows from the equation for the displacement at the crack tip, w_c

$$w_c = \frac{4a_o}{\pi E^*} S_c \ln\left(\frac{a}{a_o}\right), \quad (8a)$$

which is derived from Equation 2. Substituting for S_c from Equation 5a yields

$$w_c = \left(\frac{4a_o}{\pi E^*}\right)\left[\frac{\pi\sigma_\infty}{2\cos\frac{a_o}{a}}\right] \ln\left(\frac{a}{a_o}\right). \quad (8b)$$

Differentiation of Equation 8b with respect to the crack length a gives, for the case of interest here where $a_o/a \ll 1$ (typically $a/a_o \simeq 1/3$), $dw_c/da < 0$ as experimentally observed.

4.3. Observations on crack growth with increasing strain

A second set of experiments was undertaken to analyse the propagation of the crack into the deformation zone as the strain was sequentially increased. The strain increments were made at approximately 2 min intervals and thus the

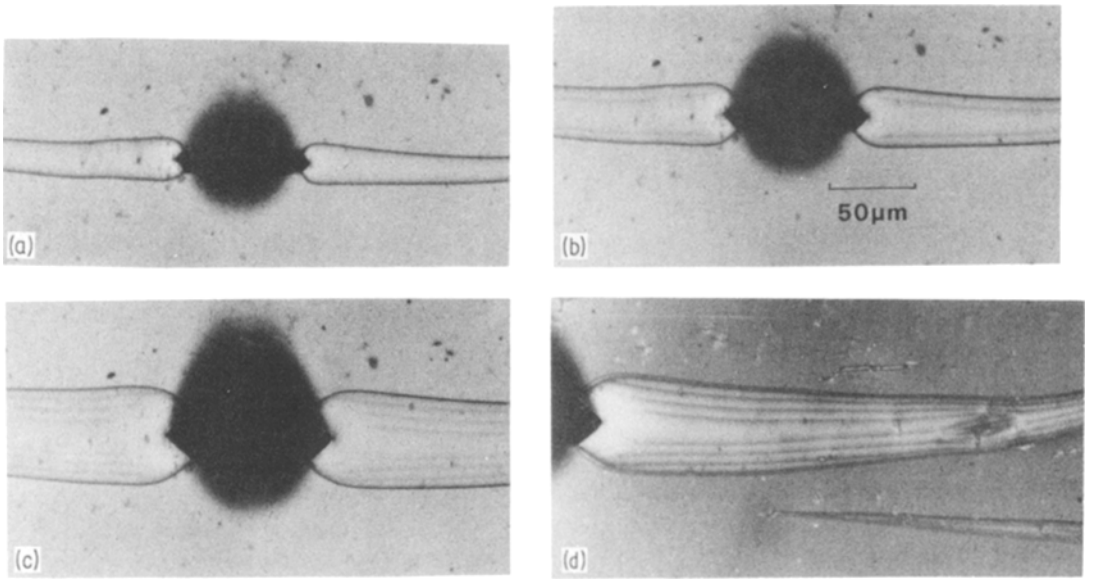

Figure 6(a to c) Crack propagation into a DZ in annealed PC as the strain is sequentially increased, (d) the same as in Fig. 6c observed in monochromatic light.

measurements recorded will not necessarily correspond to the equilibrium state.

Typical sets of micrographs showing the changing crack shape are displayed in Figs 6 and 7 for the annealed and unannealed specimens. For both the annealed and unannealed specimens it can be seen that a pronounced half "diamond" crack-tip shape is formed, with the angle subtended at the tip of the diamond decreasing with time. This result demonstrates that the crack propagates correspondingly faster than it opens.

For the case of the annealed specimens, successive stages of accelerated zone thickening due to the abrupt increase in applied strain are delineated by lines of changed contrast tracing the outer edge of the zone at the time of strain increase. These are most clearly seen in Fig. 6d, which was taken with monochromatic light. The origin of these lines will be discussed in a subsequent paper.

The effect of annealing PC on the nature of the diamond cavity produced does not seem to be very great. This result suggests that, although the strain is much less localized in the unannealed PC, in the

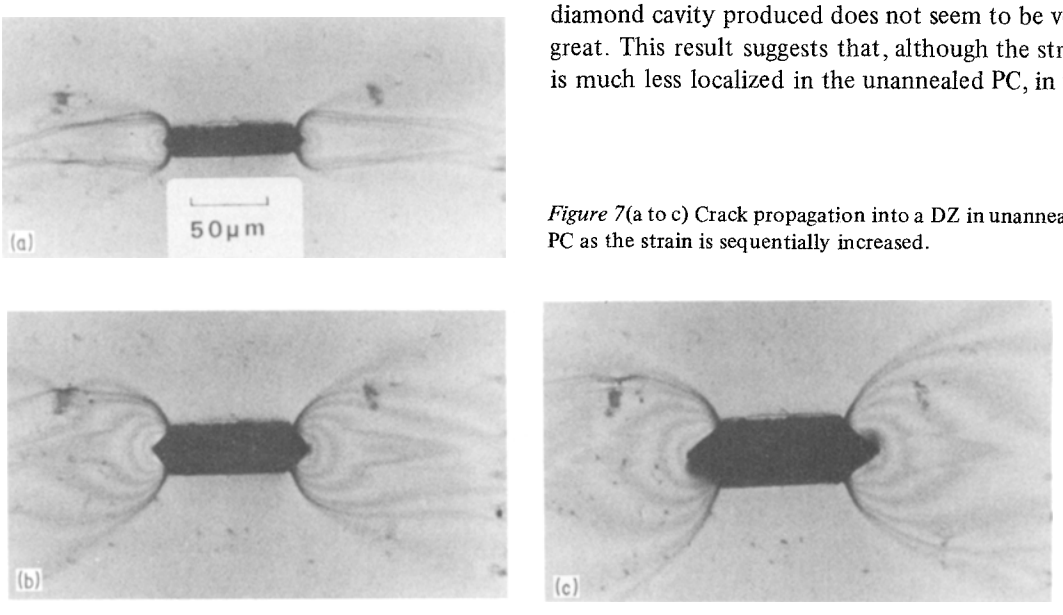

Figure 7(a to c) Crack propagation into a DZ in unannealed PC as the strain is sequentially increased.

immediate vicinity of the crack tip where there is the largest strain concentration, the plastic deformation and orientation behaviour is similar. Reinforcing this view is the fact that the local v_f at the crack tip in the two types of samples have been shown to be similar (~0.5) despite the differences elsewhere in the deformation zone. One can argue that following yielding the differences in molecular parameters introduced by the annealing process are eliminated as the polymer chains take up new configurations corresponding to a "yielded state" common to annealed and unannealed PC alike. This hypothesis is consistent with the observations of Adam *et al.* [16] who found that the enthalpy relaxation that developed during the annealing process was eliminated following yielding. However they associated this behaviour with a breakdown of the "nodular" structure [17] formed upon annealing, the evidence for which must be regarded as tenuous (e.g. [18]).

A second possible explanation for the similarity is that the method of producing the crack in the microprobe causes a local temperature rise sufficient to "anneal" the material immediately adjacent to the crack. That this cannot be the true explanation (although such a local temperature rise may occur and cause some contribution to the effect) can be verified by using a Tukon microhardness indentor to produce the starter crack [7]. Although, as discussed, this method has the disadvantage of causing a local build-up of polymer adjacent to the crack, exactly the same type of diamond crack propagation was observed as successively higher strains were applied to the specimen.

Haward and co-workers [19–22] have observed the growth of diamond-shaped cavities in a range of glassy oriented polymers. These include PC under suitable testing conditions, typically elevated temperatures and low strain rates. This growth is associated with "plastic fracture" in which a substantial amount of energy is absorbed in plastic deformation away from the immediate vicinity of the crack tip. As discussed by Cornes, Smith and Haward [20], whereas brittle fracture occurs in thermoplastics exhibiting strain softening prior to general yield (with the plastic strain localized within thin crazes or shear bands), plastic fracture is observed after yield in materials with significant orientation hardening.

More recently [23] it has been pointed out that such diamonds are embedded in a highly anisotropic matrix. Furthermore these workers have demonstrated that around a diamond cavity further deformation occurs primarily by simple shear. In their model it is envisaged that near the diamond the polymer chains shear parallel to the orientation direction until strain hardening causes a neighbouring region to yield in preference to further shear of the original. Each element is therefore strained equally, the cavity is constrained to have linear sides and the characteristic diamond is formed.

There is clearly a close similarity between the growth of diamond cavities within the neck of a drawn polymer and the propagation of a half diamond crack into the DZs described here. From the bi-refringence measurements [1] it is clear that, as with a diamond crack in a cold-drawn neck, the crack is embedded in an anisotropic (highly oriented) matrix, within which a high degree of orientation hardening has occurred. (This latter property is demonstrated by the fact that when it has deformed to a draw ratio corresponding to a v_f ~0.7 little further drawing occurs for small increases in stress.) However, careful analysis of the nature of the molecular orientation shows significant differences between the results obtained here and those reported by Walker *et al.* [23] on diamond cavities in bulk specimens. By observing the deformation of a rectangular grid of gold–palladium alloy deposited onto a fine copper mesh masking the polymer under study, Walker *et al.* [23] studied the strain field around the growing diamond cavity. For the case of PVC they reported that the maximum principal elongation remained within 5° of the draw direction everywhere, suggesting that the molecular orientation is not appreciably altered by the simple shear deformation they observed. However analysis of the molecular orientation in the DZs [1] has shown that there is a significant rotation within the lobes of the zone relative to the draw direction, the angle of rotation being as large as 30°. The details of the nature of the changes in orientation are shown in Fig. 7a of [1]. Clearly a complex pattern of deformation is occurring here, which cannot be described solely by simple shear.

At the edge of the DZ it has been shown that the direction of orientation follows the major principal stress axis, but for a sufficiently large lobe this "boundary condition" should not markedly affect the orientation around the crack itself. At first sight it would seem that there are no boundary

conditions acting in the neck of the drawn polymer described by Walker *et al.* [23] which could affect the orientation, and thus that the two sets of results are incompatible. However, a comparison of Figs 4 and 6 of [23] shows that the deformation process is altered for an "edge diamond", i.e. a diamond formed from a notch at the edge of a specimen. In this case the top and bottom "corners" of the diamond correspond to free surfaces, whereas in a true diamond cavity, growth of these corners is constrained by the surrounding polymer. The effect of the free surfaces is to permit more molecular flow normal to the draw direction with the result that there is a significantly greater rotation of the orientation axis away from the draw direction towards the direction of the diamond edge. This case corresponds much more closely to the results described here. For the DZs in annealed PC the two half "diamonds" growing at the ends of the crack are widely separated by unoriented material, which does not constrain the crack growth in the same way as a diamond cavity growing in a neck.

From this discussion it can be concluded that the diamond crack growth reported here resembles edge diamond growth more closely than the growth of full diamonds reported by Walker *et al.* [23]. Clearly the anisotropy of the matrix into which the crack is propagating is of prime importance but the claim that the polymer is deforming primarily by simple shear is an oversimplification, since the nature of the deformation they observe around diamond cavities is significantly affected by the geometry.

As can be seen in Fig. 6a to c, as the strain is increased the angle subtended at the tip of the diamond decreases. Walker *et al.* [23] report that the diamond appears to maintain its shape with time, simply becoming magnified. However, from the earlier work of Cornes *et al.* (Fig. 5 of [20]) it would appear that a reduction in angle at the diamond tip does occur with increasing strain for PVC. The geometry of the crack in this earlier work is hexagonal, rather than the true diamond of the work of Walker *et al.*, and consequently is similar to the shape of the crack described in this paper. Again this suggests that the conclusions drawn by Walker *et al.* [23] are affected by the geometrical constraints of the specimen. The changing shape of the diamond must reflect the response of the already oriented material to the changing stress field generated by the growing diamond. A detailed analysis would require a full understanding of the anisotropy of flow.

4.4. Comparison of the mechanics of deformation zones and crazes

It is of interest to compare the mechanics of the DZs in annealed PC both with crazes in other polymers (e.g. PS) and with the predictions of the Dugdale model. If the mechanical properties of DZs and crazes can be shown to be similar, then information from DZ growth experiments can be used to model craze growth. Such models would be useful because the fine scale of crazes requires the use of electron microscopy to observe their mechanical properties, but since the electron irradiation which occurs during TEM changes the properties of PS, growth experiments in which sequential craze microstructures are observed are not possible.

The most obvious difference between crazes and DZs is that the latter possess no fibril or void structure. This difference will be of prime importance in considering the response of the polymer to potentially harmful environments, and will also affect the ability of the deformed polymer to bear shear stresses. However, for other properties the absence of voids may be of lesser importance.

It has been shown that DZs grow along a minor stress trajectory, with the polymer chain orientation lying along the major principal stress axis. This directional growth is exactly analogous to the behaviour of crazes. Furthermore the surface stress profile along the zone is closely similar to that borne by a craze; it is reasonably constant over the majority of the zone with a stress concentration at the zone tip. The displacement profiles for the craze and DZ are also similar and it has been shown that both thicken by surface drawing and not by creep of the already drawn material. In contrast to these similarities, a significant difference may be observed in the extension ratio profiles, the craze having a maximum value for λ at the tip, whereas the DZ shows a λ profile which decreases monotonically near the tip. This difference is also reflected in the absence of a midrib in the DZ. It is evident also that the actual mechanism of zone tip advance must be different from that for craze tip propagation, the appropriate mechanism for the latter having been shown to be the meniscus instability [24–26] which gives rise to the fibrillated craze structure. However, the difference in mechanism may not be as great as it seems at first sight.

Ahead of the craze tip, deformation prior to fibrillation is localized in the two surfaces appearing as the presence of two "surface grooves" [25,26], typically ~25 nm deep for crazes in PS. As the thickness of the film is decreased, lateral constraint through the film thickness is relaxed and the percentage thickness occupied by the surface grooves increases. Together these effects lead to the suppression of fibrillation and the craze structure in PS films ~100 nm thick no longer comprises a fibril/void structure with ~6 nm fibrils, but more closely resembles a perforated sheet [27]. This sheet structure arises from the intermittent coalescence of the surface grooves without the development of the meniscus instability.

A logical extension of this mechanism in very thin films is to visualize a drawn zone corresponding to the two surface grooves extending throughout the film thickness, without the presence of voids. This is precisely the observed form of the DZ. Since it is known that plane stress deformation occurs over a far wider range of thickness for PC than for PS, it seems plausible that the coalescence of surface grooves may similarly extend up to much higher film thickness; for these, intermittent void formation apparently does not occur.

Thus it would seem that the mechanical properties of DZ's and crazes are closely similar and that the experimental results on DZs may be used to infer properties of crazes. For instance these experiments permit verification of the intuitive idea that the surface stress $S(x,t)$ (the stress producing drawing at the edge of the DZ or the surface of the craze) must decrease during growth. It has also been shown that the rate of DZ thickening follows the changing value of the surface stress, i.e. dw/dt increases as $S_c(x,t)$ increases.

Secondly, it is worth considering how well the simple Dugdale model fits the experimental data. Previous workers [2,3] have claimed good agreement between craze profiles and the Dugdale model, using optical interference microscopy. From the results presented above (Fig. 3a and b) it is clear that in detail the experimental displacement profile does not agree with the Dugdale model. However, it is also clear (Fig. 4) that the surface stress is nearly constant over the majority of the zone despite this changed $w(x)$ profile. Similarly, the observed decrease in (w_0/a) with time is at least qualitatively predicted by the Dugdale model. It has previously been demonstrated [7] that the difference between the fracture toughness G_{Ic} calculated from the Dugdale model and using the actual experimental data for crazes in PS is small. Thus it seems that, despite the discrepancies in fine detail between the model and experimental results (both for crazes and DZs), the Dugdale model is nevertheless a good approximation for most properties.

5. Conclusions

The following conclusions about deformation at crack tips in PC can be drawn:

(1) In annealed PC, well-defined flame-shaped zones of drawn but unvoided material are formed. Within these zones an approximately constant value of $v_f \sim 0.71$ is obtained.

(2) A high degree of molecular orientation occurs within the zone, giving $\Delta n = 0.117$. For the majority of the zone the molecular chains lie along the draw direction.

(3) In unannealed PC, a much more diffuse zone of deformation is formed. Within this zone there is a gradual change in both v_f and molecular orientation.

(4) Analysis of the micromechanics of the DZ in annealed PC shows that both the displacement profile and the surface stress are in reasonable agreement with the predictions of the Dugdale model.

(5) A comparison of the local displacement rates with the form of the surface stress shows that the rate is a sensitive function of the local stress, the rate dropping rapidly during growth as the average stress along the zone decreases.

(6) As higher levels of strain are applied to the specimen, crack propagation into the DZ occurs with a characteristic diamond shape.

Acknowledgements

The financial support of the US Army Research Office at Durham is gratefully acknowledged. This research has also benefited from the use of the facilities at the Cornell Materials Science Center which is funded by the National Science Foundation. We would like to thank Dr Roger Kambour for supplying the Lexan resin and Professor R. N. Haward for communicating results to us prior to publication.

References

1. A. M. DONALD and E. J. KRAMER, *J. Mater. Sci.* **16** (1981) 2967.
2. H. R. BROWN and I. M. WARD, *Polymer* **14** (1973) 469.
3. G. N. WEIDMANN and W. DÖLL, *Colloid Polymer*

Sci. **254** (1976) 205.
4. S. J. ISRAEL, E. L. THOMAS and W. W. GERBERICH, *J. Mater. Sci.* **14** (1979) 2128.
5. D. S. DUGDALE, *J. Mech. Sol.* **8** (1960) 100.
6. B. D. LAUTERWASSER and E. J. KRAMER, *Phil. Mag.* **39A** (1979) 469.
7. T. CHAN, A. M. DONALD and E. J. KRAMER, *J. Mater. Sci.* **16** (1981) 676.
8. N. VERHEULPEN-HEYMANS, *Polymer* **20** (1979) 356.
9. J. N. GOODIER and F. A. FIELD, Proceedings of the International Conference on Fracture of Solids, edited by D. C. DRUCKER and J. J. GILMAN, Met. Soc. Conferences, Vol. 20 (Interscience, New York, 1963) p. 103.
10. I. N. SNEDDON, "Fourier Transforms", (McGraw Hill, New York, 1951) p. 395.
11. N. VERHEULPEN-HEYMANS and J. C. BAUWENS, *J. Mater. Sci.* **11** (1976) 117.
12. B. A. BILBY and J. D. ESHELBY, in "Fracture", Vol. I, edited by H. LIEBOWITZ (Academic Press, London and New York) p. 111.
13. N. VERHEULPEN-HEYMANS, *Polymer* **21** (1980) 97.
14. B. N. DEY, *J. Appl. Phys.* **38** (1967) 4144.
15. E. J. KRAMER, *J. Appl. Phys.* **41** (1970) 4327.
16. G. A. ADAM, A. CROSS and R. N. HAWARD, *J. Mater. Sci.* **10** (1975) 1582.
17. M. G. WYZGOSKI and G. S. Y. YEH, *Int. J. Polymer Mater.* **3** (1974) 133.
18. D. R. UHLMANN, *Discuss. Faraday Soc.* **68** (1979) 68/5.
19. P. L. CORNES and R. N. HAWARD, *Polymer* **15** (1974) 149.
20. P. L. CORNES, K. SMITH and R. N. HAWARD, *J. Polymer Sci. Polymer Phys. Ed.* **15** (1977) 955.
21. N. WALKER, J. N. HAY and R. N. HAWARD, *Polymer* **20** (1979) 1056.
22. N. WALKER, R. N. HAWARD and J. N. HAY, *J. Mater. Sci.* **16** (1981) 817.
23. *Idem, ibid.* **14** (179) 1085.
24. G. I. TAYLOR, *Proc. Roy. Soc.* **A201** (1950) 192.
25. A. S. ARGON and M. M. SALAMA, *Phil. Mag.* **36** (1977) 1217.
26. A. M. DONALD and E. J. KRAMER, *ibid.* **43A** (1981) 857.
27. A. M. DONALD, T. CHAN and E. J. KRAMER, *J. Mater. Sci.* **16** (1981) 669.

Received 27 February and accepted 26 March 1981.